Turkish Journal of Electrical Engineering & Computer Sciences

http://journals.tubitak.gov.tr/elektrik/

Research Article

Turk J Elec Eng & Comp Sci
(2021) 29: 773 – 795

doi:10.3906/elk-2003-46

Optimal planning DG and BES units in distribution system considering uncertainty of power generation and time-varying load

Mansur KHASANOV[1], **Salah KAMEL**[2], **Ayman AWAD**[2,3], **Francisco JURADO**[3,*]
[1]State Key Laboratory of Power Transmission Equipment and System Security and New Technology, Chongqing University, Chongqing, China
[2]Department of Electrical Engineering, Faculty of Engineering, Aswan University, Aswan, Egypt
[3]Department of Electrical Engineering, University of Jaén, Jaén, Spain

Received: 08.03.2020 • **Accepted/Published Online:** 20.10.2020 • **Final Version:** 30.03.2021

Abstract: Global environmental problems associated with traditional energy generation have led to a rapid increase in the use of renewable energy sources (RES) in power systems. The integration of renewable energy technologies is commercially available nowadays, and the most common of such RES technology is photovoltaic (PV). This paper proposes an application of hybrid teaching-learning and artificial bee colony (TLABC) technique for determining the optimal allocation of PV based distributed generation (DG) and battery energy storage (BES) units in the distribution system (DS) with the aim of minimizing the total power losses. Besides, some potential nodes identified by the power loss sensitivity factor (PLSF). Thereupon TLABC is applied to determine the location of the DG and its size from the candidate nodes. The beta probability distribution function (PDF) is employed to characterize the randomness of solar radiation. High penetration of RES can lead to a high level of risk in DS stability. To maintain system stability, BES is considered to smooth out the fluctuations and improve supply continuity. The benefits of using BES is mainly dependent on operational strategies related to PV and storage in DS. The performance of the developed approach is tested on the 69 node and 118 node DSs and compared with the differential evolution (DE) algorithm, genetic algorithm (GA), for a fair comparison. Besides, the developed approach compared with other methods in literature which are solved the same problem. The results show how practical is the developed approach compared with other techniques.

Key words: Distributed generation, optimization, battery energy storage, energy loss, uncertainty

1. Introduction

In the last few years, considerable attention has been paid to the usage of RES (such as PV, wind, etc.) to minimize power losses due to global environmental problems associated with traditional generation. Many countries have been introduced or are proceeding towards the implementation of renewable energy policies like the renewable energy portfolio standard (RPS) [1]. Accepting an RPS is a production obligation of a certain percentage of the total electricity production from RES for a specific date. However, available PV energy is unstable and variable. However, high PV integration can lead to large power fluctuations, which may risk the provision of continuous power supply. In addition, the amount of PV energy that can be absorbed by the power system at a particular time may be significantly limited, since the available traditional units may not be able to respond to changes caused by PV units' fluctuations. To use this source of energy as a viable source, as well as to ensure system stability, BES are used to retain violations of system constraints and decrease power

*Correspondence: Correspondence: fjurado@ujaen.es

fluctuations in DS [2]. Thus, the optimal allocation of PV units can improve system reliability and efficiency by solving their variable nature problems [3]. The optimal allocation of PV units in the system is essential; therefore, unplanned distribution can have many adverse effects on the system [4]. To date, many previous studies have been focused on the optimal solution to the problem. Metaheuristic based optimization methods have been implemented to solve DG allocation problems, such as the adaptive genetic algorithm (AGA) [5], the multiobjective quasi-oppositional teaching learning-based optimization (QOTLBO) and quasi-oppositional swine influenza model-based optimization with quarantine (QOSIMBO-Q) [6], the bat algorithm (BA) and particle swarm optimization (PSO) [7], stochastic fractal search algorithm (SFSA) [8], a mixed integer nonlinear programming (MINLP) technique [9] and krill herd algorithm (KHA) [10]. Mansur et al. have introduced a tree growth programming method for optimal allocation of DGs in the DS in terms of minimizing annual power losses in [11].

While most of the researches are focusing on the autonomous PV power generation system, several researches analyse the grid-connected hybrid system (HS). Santos et al. have studied how grid dependence is influenced when the RES is integrated in accordance with the relationship between the load and probabilistic RES generation. The study showed that the combination of DG units reduces importing power from the grid and, prevents losses in large-scale imported power through a substation [12]. Determining the optimal size for PV with a BES, and the best combination (penetration of source) in HS has been investigated in [13]. Power flow and related power losses due to the influence of HSs with the grid have been also examined [13]. A charge and discharge strategy of BES units have been presented to mitigate the unexpected changes in PV outputs, and residential systems peak loads support in the evening [14]. Efficient voltage regulation in DSs has been achieved by management of the BES units' output on the consumer side with high PV penetration [15]. Finally, an optimal discharge and charge scheduling of the BES unit for DSs integrated the sizeable PV-based DG outputs with aiming energy loss minimization has been studied in [16]. Nevertheless, the technical impacts of the RES based DGs have not been properly addressed in such studies.

This paper presents a more accurate optimization approach based on teaching-learning and artificial bee colony (TLABC) and Power loss sensitivity factor (PLSF)PLSF for optimal allocating the PV and BES units into a DS. The main objective function is energy loss minimization. In addition, the voltage stability index (VSI) is calculated to show the performance of the proposed method on the stability of DS.

PLSF has been applied to determine the potential nodes whereof more suitable to be connected with PV and BES units, then the optimal allocations of DG and BES are determined using TLABC. The Beta PDF is employed to depict the randomness of solar radiation. BES is considered to smooth out the fluctuations and improve supply continuity. The performance of the developed approach is tested on the 69 node and 118 node DSs and compared with GA [17], DE [18] and other techniques in the literature.

The remaining of this paper is arranged as follows: Section 2 describes PLSF analysis. Probabilistic power generation of PV based DG, BES and load modeling are presented in Section 3. The mathematical formulation and optimal PV and BES sizing presented in Section 4. Section 5 describes the proposed approach and its implementation steps. Section 6 describes the simulation results. Conclusions are mentioned in Section 8.

2. Power loss sensitivity factor (PLSF)

In this study, PLSF is used to determine the candidate nodes whereof more compatible for connecting the DG. This strategy is more helpful to decrease the search space. The equivalent grid-connected radial DS is shown in Figure 1.

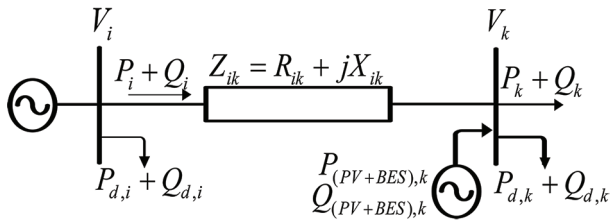

Figure 1. Equivalent radial distribution system diagram.

In Figure 1, P_i and P_k represent the active power injected at node i and node k, respectively. Q_i and Q_k represent the reactive power injected at node i and node k, respectively. V_i and V_k are the voltage magnitudes of node i and node k, respectively. X_i and X_k represent the reactance and resistance of branch ik, respectively. P_i and P_k and $P_{DG+BES,k}$ and $Q_{DG+BES,k}$ represent the active and reactive power of DG+BES added at node k, respectively. $P_{d,i}$, $Q_{d,i}$, $P_{d,k}$ and $P_{d,k}$ are the active and reactive load at node i and node k, respectively. The active and reactive power losses of branch ik are calculated as:

$$P_{ik-loss} = \frac{({P_k}^2 + {Q_k}^2)^* R_{ik}}{V_k^2}, \tag{1}$$

$$Q_{ik-loss} = \frac{({P_k}^2 + {Q_k}^2)^* X_{ik}}{V_k^2}. \tag{2}$$

Accordingly, minimizing the total active power losses in the DS leads to reduce the total active energy losses E_{loss} during 24 h as:

$$E_{loss} = \sum_{t=1}^{24} P_{ik-loss}(t)\Delta t, \tag{3}$$

where Δt is the time duration, which is 1 h in this study.

PLSF can calculate using (4) as shown in Figures 2 and 3.

$$\frac{\partial P_{ik-loss}}{\partial Q_k} = \frac{2{Q_k}^* R_{ik}}{(V_k)^2} \tag{4}$$

After calculating PLSF values of all nodes, they are arranged in descending order as per these values. The ranked up to 50% PLSF values of nodes can be regarded as candidate nodes for optimal integration of PV and BESs in DS [19-22]. In this study, 34 and 58 nodes have been selected as candidate buses for 69-node and 118-node test systems, respectively. Due to space limitation, we will not show all candidate buses here.

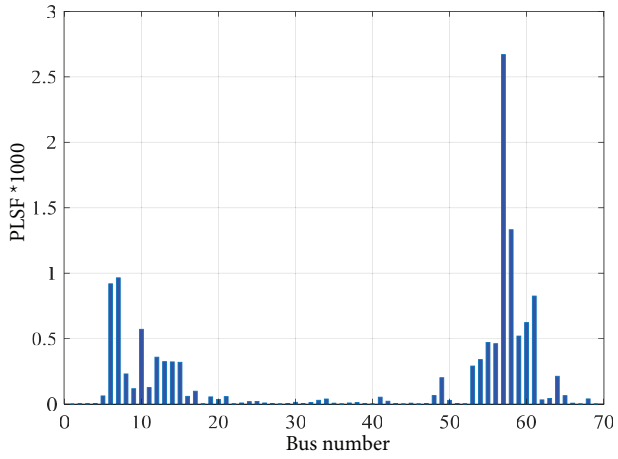

Figure 2. Determined values by PLSF for 69 node distribution system.

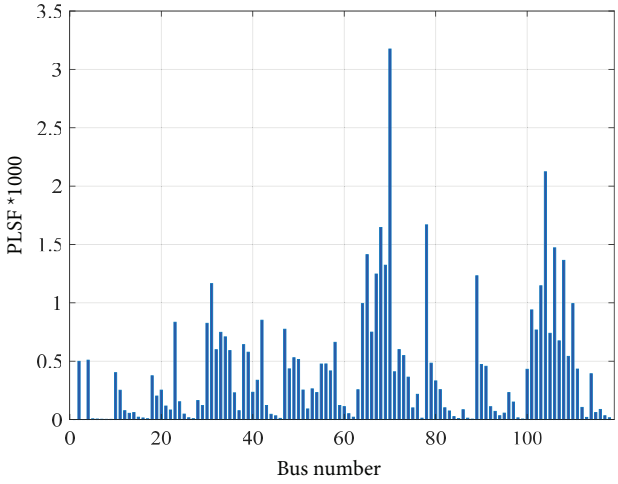

Figure 3. Determined values by PLSF for 118 node distribution system.

3. PV, BES and load models

3.1. PV modeling

Power generation using PV unit is highly dependent on meteorological conditions, such as solar radiation, and ambient temperature. These conditions are directly related to geographic area. Hence, the effectiveness of the conditions of solar radiation in a certain area is usually analyzed at the initial stage for the effective use of PV panels.

The standard deviation (SD) and mean of hourly solar radiation per day is calculated using collected historical data. Continuous PDF for an exact time interval is divided into stages, in each solar radiation within certain limits. The PV power generation is determined by all possible stages of probability's in that hour. In this study, the step for solar radiation is 0.05 kW/m2. The average value of each stage is used as output power calculation for this stage (i.e. if the first stage of solar irradiation, is between 0 kW/m2 and 0.05 kW/m2, the average value of this stage is 0.025 kW/m^2).

3.1.1. Solar radiation model

It is considered that the probabilistic nature of solar radiation follows the beta PDF [23]. The beta PDF of solar radiation 's' (kW/m^2) in the time interval 't' is defined as:

$$f_b(s^t) = \frac{\Gamma(\alpha^2+\beta^2)}{\Gamma(\alpha^2)\Gamma(\beta^2)}, 0 \le S^t \le 1, \alpha^t, \beta^t \ge 0 \tag{5}$$

$$otherwise: f_b(s^t) = 0 \tag{6}$$

where, $f_b(s^t)$ is the Beta PDF of s^t, α^t and β^t are the shape rates of Beta PDF and Γ depicts Gamma function. The shape rates of Beta PDF can be found using mean (μ) and SD (σ) of radiation for suitable time interval.

$$\beta^t = (1-\mu^t)(\frac{\mu^t(1+\mu^t)}{\sigma^{t2}} - 1); \alpha^t = \frac{\mu^t * \beta^t}{1-\mu^t} \tag{7}$$

The PV array hourly average power output corresponding an exact time interval 't' (P_{pv}^t) is expressed as (8). A typical day for three years is generated in p.u., as shown in Figure 4.

$$P_{pv}^t = \sum_{g=1}^{n_s} P_{pv_o}(s_g^t) f_b(s_g^t), \tag{8}$$

where 'g' denotes a stage factor and n_s is the solar radiation discrete stage number. s_g^t is the g^{th} stage of solar radiation at t^{th} time interval.

Solar radiation and ambient temperature are the basic dominant factors that affect the PV array power output. The PV power generation with average solar radiation (s_{ag}) for the g^{th} stage is estimated as [23]:

$$P_{pv_o}(S_{ag}) = N_{pv_{mod}} * FF * V_g * I_g, \tag{9}$$

where

$$FF = \frac{V_{MPP} * I_{MPP}}{V_{OC} * I_{SC}}; V_g = V_{OC} - K_v * T_{cg}; I_g = S_{ag}[I_{SC} + K_i(T_C - 25)]; T_{cg} = T_A + S_{ag}[\frac{N_{OT}-20}{0.8}]. \tag{10}$$

Here, $N_{pv_{mod}}$ is PV modules total number. T_A is ambient temperature; V_{MPP} and I_{MPP} are maximum power tracing voltage (V) and current(A), respectively; V_{OC} and I_{SC} are open circuit voltage and short circuit current, respectively; K_i and K_v are current and voltage temperature coefficients(A/C and V/C) respectively; FF is the fill factor; T_{cg} is PV module temperature at g^{th} stage.

3.2. BES modeling

Over the last few years, several types of energy storage (ES) have been intensively studied. These types include super capacitors, electrochemical battery, compressed air ES, flywheel ES, and superconducting magnetic ES.

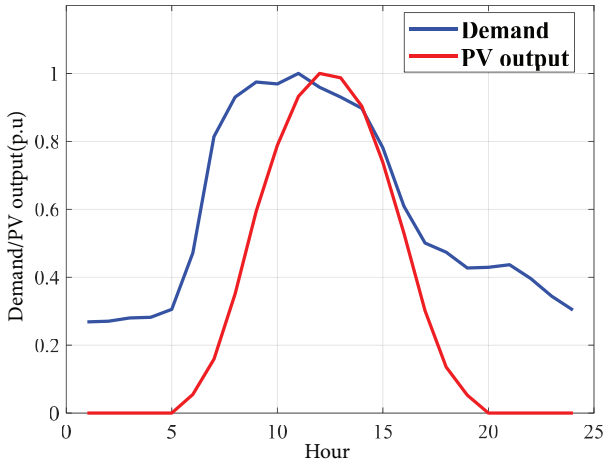

Figure 4. Normalized daily active load curve and PV output.

For this paper lithium-ion (Li-ion) BES is selected with a roundtrip efficiency of 77%. This is the most popular type of BES for today's portable electronics, characterized by the best energy and weight ratio, no memory effect, and no slow charge loss on nonuse. However, incorrect handling may cause a Li-ion battery to explode. Lithium-ion BES is becoming increasingly popular with defense, aerospace and automotive applications due to its high energy intensity. The charging and discharging equations of the BES are given in (11) and (12).

$$Discharge: E_{BES_k}(t+1) = E_{BES_k}(t) - \Delta t \frac{P^{disch}_{BES_k}}{\eta_d} \tag{11}$$

$$Charge: E_{BES_k}(t+1) = E_{BES_k}(t) - \Delta t * P^{ch}_{BES_k} * \eta_c \tag{12}$$

where, $P^{disch}_{BES_k}$ is the discharged power by the BES for a t time duration, $P^{ch}_{BES_k}$ is the power charged by the PV to the BES, that is, the BES is being charged. $E_{BES_k}(t)$ is the energy stored in the BES at time (t). Δt is time duration of each segment. η_d and η_c are the discharging and charging efficiency, respectively.

BES must satisfy the restrictions given in (13) to (16). Power limits:

$$0 \leq P^{disch}_{BES_k} \leq P^{disch,max}_{BES_k} \tag{13}$$

$$0 \leq P^{ch}_{BES_k} \leq P^{ch,max}_{BES_k} \tag{14}$$

Stored energy limits:

$$E_{BES_kmin} \leq E_{BES_k}(t) \leq E_{BES_kmax} \tag{15}$$

Starting and ending energy limits:

$$E_{BES_k}(0) \leq E_{BES_k}(T) \leq E_{BES_ks}, \tag{16}$$

where $P_{BES_k}^{disch,max}$ is the maximum discharge power rate; $P_{BES_k}^{ch,max}$ is the maximum charging power rate; E_{BES_kmin} and E_{BES_kmax} are the lower and upper energy limits of the BES; $E_{BES_k}(0)$ is initial energy of the BES; E_{BES_ks} is the BES unit initial limit of stored energy. For the energy balance, the stored energy $E_{BES_k}(T)$ is set the same as the initial stored energy. In this paper, minimum and maximum capacity limits of BES units are assumed to be 20% and 90%, respectively [23].

3.3. Load model

The load demand for the system is modeled corresponding to the normalized daily 24-h load curve with a peak of 1 pu, as shown in Figure 4 [24]. The load factor (LF) can determined as the field beneath the load curve, the load curve in p.u. subdivide by the sum of time interval [24].

$$LF = \sum_{T=1}^{24} \frac{p.u.Demand(t)}{24} \tag{17}$$

The voltage-dependent load demand model, which includes variable load over time, can be calculated as [24]:

$$P_k(t) = P_{ok}(t) * V_k^{n_p} \tag{18}$$

$$Q_k(t) = Q_{ok}(t) * V_k^{n_q}, \tag{19}$$

where P_k and Q_k represent active and reactive power injected at node k. P_{ok} and Q_{ok} represent the active and reactive power loads at node k. V_k represents the voltage value at node k, and n_p and n_q represent active and reactive load voltage indexes, respectively [24], where $n_p = 1.51$ and $n_q = 3.4$.

4. Mathematical formulation of the studied optimization problem

4.1. Objective function

In this study, optimal allocating of PV and PV+BES units with aim minimize energy loss using the developed approach. This objective function (OF) is calculated as follows:

$$F_{obj} = minimize(P_{loss}) * \Delta t = minimize(E_{loss}), \tag{20}$$

where E_{loss} is the total energy loss. The VSI is used for indicating the voltage stability of DS. High VSI of any node identifies the less sensitive node to the voltage collapse. The VSI of node k is calculated as follows [11]:

$$VSI(k) = |V_i|^4 - 4(P_k X_{ik} - Q_k R_{ik})^2 - 4|V_i|^2(P_k R_{ik} - Q_k X_{ik}) \tag{21}$$

The OF is subjected to some constraints such as DG size, node voltage and branch capacity limitation.

4.2. Equality constraints

The sum of injected and outgoing powers must be equal:

$$P_{slack} + \sum_{i=1}^{N_{DG}} P_{DG}(i) = \sum_{i=1}^{L} P_{lineloss}(i) + \sum_{k=1}^{N} P_d(k) \tag{22}$$

$$Q_{slack} + \sum_{i=1}^{N_{DG}} Q_{DG}(i) = \sum_{i=1}^{L} Q_{lineloss}(i) + \sum_{k=1}^{N} Q_d(k) \tag{23}$$

where, P_{slack} and Q_{slack} represent active and reactive power of slack node. N_{DG} is installed DG units' number, L is total branch number.

4.3. Inequality constraints

4.3.1. Voltage constraint

The magnitude of each node voltage must be limited as:

$$V_{lb} \leq |V_i| \leq V_{ub} \tag{24}$$

where, V_{lb} and V_{ub} represent minimum and maximum voltage magnitudes.

4.3.2. DG's power constraint

The installed DG size must be limited as [11]:

$$P_{DG}^{min} \leq P_{DG} \leq P_{DG}^{max} \tag{25}$$

$$Q_{DG}^{min} \leq Q_{DG} \leq Q_{DG}^{max} \tag{26}$$

where P_{DG}^{min} and P_{DG}^{max} represent the maximum and minimum DG units' active power, respectively. Q_{DG}^{min} and Q_{DG}^{max} represent the maximum and minimum DG units' reactive power, respectively.

4.3.3. Branch capacity limitation

The branch capacity must meet the following limitation:

$$S_{Li} \leq S_{Li(rated)} \tag{27}$$

4.4. Determining the size of the combination of PV and BESs (PV+BES)

4.4.1. PV sizing

Figure 5 shows the grid-connected hybrid PV+BES conceptual model. This model is designed for installation on the roofs of commercial premises. The concept is to convert every nonmanageable PV unit output to a manageable PV unit with a collaboration of PV and BES units, in order to minimize system total power losses

for a given load. This strategy can generate a diurnal quantity of manageable energy, $E_{(PV+BES)}$. The E_{PV} is PV unit generating energy, during the 24-h cycle of the day. $E^g_{PV}rid$ is transferred energy to the grid. The PV unit's excess energy is used to charge the BES unit, $E^c_{BES}h$, instead of cutting it when PV unit output power is bigger than load during the day. When the output power of PV unit is low or zero overnight, then the stored energy is discharged to the system, $E^d_{BES}isch$. PV and BES units are located on the same node to prevent energy losses in the charge state of BES.

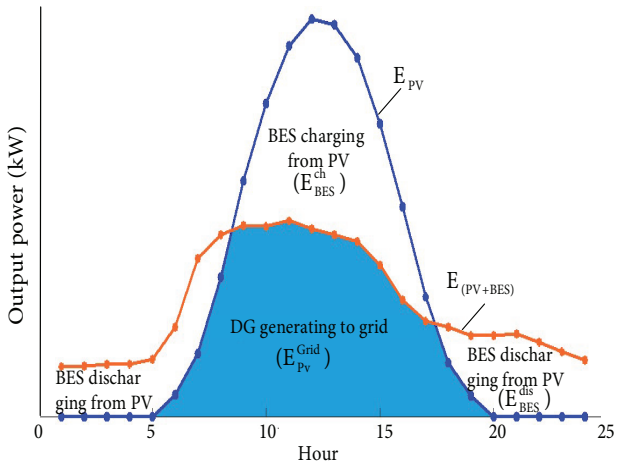

Figure 5. PV power output and BES charging and discharging performance.

The daily PV+BES unit amount of energy for all the duration (T = 24 h) on node j can be express as:

$$E_{PV+BES_k} = \sum_{t=1}^{24} P_{PV+BES}(t) * \Delta t, \tag{28}$$

where $P_{PV+BES}(t)$ is the collaboration of PV and BES unit's active power output on node k during a given day time interval t.

The daily charge and discharge energy on node j can be obtained by calculating (29) and (30) (see Figure 5).

$$E^{ch}_{BES_j} = \sum_{t=1}^{24} P^{ch}_{BES_j}(t) * \Delta t \tag{29}$$

$$E^{disch}_{BES_j} = \sum_{t=1}^{24} P^{disch}_{BES_j}(t) * \Delta t \tag{30}$$

The PV+BES and PV units' total output energy at node j can be expressed as:

$$E_{(PV+BES)_j} = E^{Grid}_{PV_j} + E^{Disch}_{BES_j} \tag{31}$$

$$E_{PV_j} = E^{Grid}_{PV_j} + E^{ch}_{BES_j}, \tag{32}$$

where $E_{PV_j}^{Grid}$ is the PV unit energy amount transferring to the system at node j. The BES unit charge and discharge energy at node k with a roundtrip efficiency ($\eta_{BES} = \eta_c \eta_d$) as follows:

$$E_{BES_j}^{Disch} = \eta_{BES} * E_{BES_j}^{ch}. \tag{33}$$

The PV unit total output energy at node j can be calculated based on (31) to (33) as:

$$E_{PV_j} = \frac{E_{(PV+BES)_j} - (1 - \eta_{BES}) E_{PV_j}^{Grid}}{\eta_{BES}}. \tag{34}$$

The maximum PV unit power generation during a certain time duration, 24-hour cycle of the day is used to indicate the PV unit nominal power or optimal PV unit size at node j.

$$P_{PV_j} = CF_{PV}^{unit} * E_{PV_j}, \tag{35}$$

where $CF_{PV}^{unit} = \frac{P_{PV}^{unit}}{E_{PV}^{unit}}$, P_{PV}^{unit} is PV unit maximum power output, and E_{PV}^{unit} is the PV unit generated energy during 24-h. Assuming $\eta_{BES} = 1$, from (35) the initial size of PV calculated as $P_{PV_k} = CF_{PV}^{unit} * E_{(PV+BES)_k}$, and $E_{PV_k}^{Grid}$ is then taken from Figure 6, for example. When $\eta_B ES$ is less than unit, P_{PV_k} increases. Therefore, the optimal size of PV is obtained from the Eqs. (34) and (35) as:

$$P_{PV_j} = CF_{PV}^{unit} (\frac{E_{(PV+BES)_j} - (1 - \eta_{BES}) E_{PV_j}^{Grid}}{\eta_{BES}}). \tag{36}$$

4.4.2. BES sizing

The optimal BES unit's size at node j is found based on the nominal power (P_{BES_j}) and energy capacity (E_{BES_j}) as well it can hold all the excess a PV unit's energy, that needs to be curtailed to keep system losses at the lowest level for each period. The upper charge and discharge power over a specific duration during the 24-hour cycle of the day are used to determine BES unit nominal power. The maximum energy of charge during this period is used to identify BES unit energy capacity.

5. Teaching-learning and artificial bee colony (TLABC)

TLABC is a hybridization of the teaching-learning (TLBO) [25] and artificial bee colony optimization (ABC)[26], which combines the benefits of both (the exploitation of TLBO and the exploration of ABC) [27]. TLABC is starting with initializing the number of population (NP), $y_i = (y_{i1}, y_{i2}, ..., y_{iD}), i \in \{1, 2, ..., NP\}$,

$$y_{ij} = y_{min,j} + (y_{max,j} - y_{min,j}) * rand, \tag{37}$$

where $y_{min,j}$ and $y_{max,j}$ represent the lower and upper bounds of the dimension j. Then calculate fitness values as:

$$fit(X_i) = \frac{1}{1 + f(X_i)}, f(X_i) \geq 0 \tag{38}$$

$$otherwise : fit(X_i) = |1 + f(X_i)|, \tag{39}$$

where, $fit(y_i)$ is fitness function value of y_i. The TLABC is effectively employed three hybrid search phases to find a global solution as follows.

5.1. Teaching-based employed bee phase

Here every employed bee search new resource of food uses hybrid TLBO teaching tactics.

$$u_{i,d} = y_{i,d}^{old} + rand_{22} * (y_{teacher,d} - T_F * y_{mean,d}), rand_1 1 < 0.5 \tag{40}$$

$$otherwise : u_{i,d} = y_{r_{11},d} + S(y_{r_{22},d} - y_{r_{33},d}), \tag{41}$$

where r_{11}, r_{22}, and $r_{33}(r_{11} \neq r_{22} \neq r_{33} \neq i)$ are integers and randomly selected from $\{1, 2, ..., NP\}; d \in \{1, 2, ..., D\}$, $rand_{11}$ and $rand_{22}$ represent random numbers [0,1]. T_F is the teacher factor. S is scale factor in [0,1]. If u_i is better than y_i , then u_i is used to substitute y_i. $y_{i,d}^o ld$ is i_{th} position of old learner. $y_{teacher,d}$ and $y_{mean,d}$ represent position of the teacher and current generation mean.

5.2. Learning-based onlooker bee stage

Here the onlooker bee chooses the sustenance resource to search out as indicated the selection probability p.

$$P_i = \frac{fit(y_i)}{\sum_{i=1}^{SN} fit(y_i)} \tag{42}$$

After that, the onlooker bee finds out new food source using the TLBO's learning tactics:

$$u_S = y_S + rand * (y_S - y_j), f(y_s) \leq f(y_j) \tag{43}$$

$$u_S = y_S + rand * (y_j - y_S), f(y_s) > f(y_j), \tag{44}$$

where $J \in \{1, 2, ..., NP\}$ and $j \neq S$. If u_S is better than y_S ,then u_S is used to substitute y_S.

5.3. Generalized oppositional scout bee phase

Here, if a nourishment resource y_i cannot be improved further for specific period time, it is viewed as depleted and would be relinquished. After that a new candidate solution randomly $y_i = (y_{i1}, ..., y_{ij}, ..., y_{iD})$ and generalized oppositional solution $y_i^{GO} = (y_{i1}^{GO}, y_{i2}^{GO}, ..., y_{iD}^{GO})$ are created:

$$y_i^{GO} = k(a_j + b_j) - y_{ij}, \tag{45}$$

where k is a random number between 0 and 1, and $a_j = max(y_{ij}), b_j = min(y_{ij})$.
The best solution of them is utilized rather than the old depleted nourishment source.

$$y_i^{GO} = y_i, f(y_i) \leq f(y_i^{GO}) \tag{46}$$

$$= y_i^{GO}, f(y_i) > f(y_i^{GO}) \tag{47}$$

Figure 6 depicts the flow chart of the developed approach.

6. Numerical results

In this section, the developed approach (hybrid TLABC with PLSF) has been validated using the 69 node and 118-node DSs. The 69-node system is a radial DS with a nominal voltage of 12.66 kV, active and reactive loads are 3801.5 kW and 2694.6 kVAr, respectively, where the incorporated loads are commercial load type. The complete system data is given in [28]. Without DG integration, the active and reactive power losses are 224.98 kW and 102.187 kVAr, respectively. The 118-node system is a large-scale radial DS with a nominal voltage of 11 kV, its active and reactive loads are 22710 kW and 17041 kVAr, respectively, where the loads are commercial load type. The complete system data is given in [29]. Without DG integration, the active and reactive power losses are 1297.95 kW and 978.54 kVAr, respectively. The mean and SD for every hour of the day is computed using historical data of solar radiation per hour [24].

The developed approach and forward-backward power flow technique has been modeled using MATLAB R2018b. To show how effective is the developed approach, the subsequent scenarios are discussed:

Scenario (1): Optimal allocation of single and multiple PV units at unity power factor for minimizing the total power losses without uncertainty in demand load.

Scenario (2): Optimal planning of PV+BES for minimizing the total energy losses and enhancing the voltage profile.

6.1. Scenario (1)

6.1.1. Simulation of 69 node DS

The main obtained results (power losses, minimum voltage, maximum voltage, VSI, cost of losses and cost of saving) using the developed technique are presented in Table 1. From this table it is seen that the total power loss is reduced to 83.222 kW, 71.674 kW and 69.426 kW (with loss reduction of 63.01%, 68.1412% and 69.141%) when one, two and three PV-based DG units are included in 69 node DS, respectively. If we take the energy cost 0.06 $, then the annual energy savings will be 74505 US dollars, 80575 US dollars and 81757 US dollars for integrated one, two and three PV-based DG units in the test DS, respectively. The minimum voltage raised from 0.90919 p.u. up to 0.96829, 0.97893 and 0.97897 p.u. for integrated one, two, and three PV-based DG units in the test DS, respectively. Minimum VSI raised from $ 0.683 up to 0.879, 0.9183 and 0.9185 p.u. for integrated one, two, and three PV-based DG units in the test DS, respectively.

As Table 2 shows, the developed approach allows the highest power loss reduction in case of installing DG units compared to other optimization approaches. Consequently, the developed approach is considered more effective and dependable wherewith reminder optimization techniques regarding the overall power loss reduction in DS.

6.1.2. Simulation of 118-node DS

The results of large-scale 118-node DS are presented in Table 3, where the optimal DG allocation is determined using the developed approach. From this table, it is seen that the total power loss is reduced to 1016.694 kW,

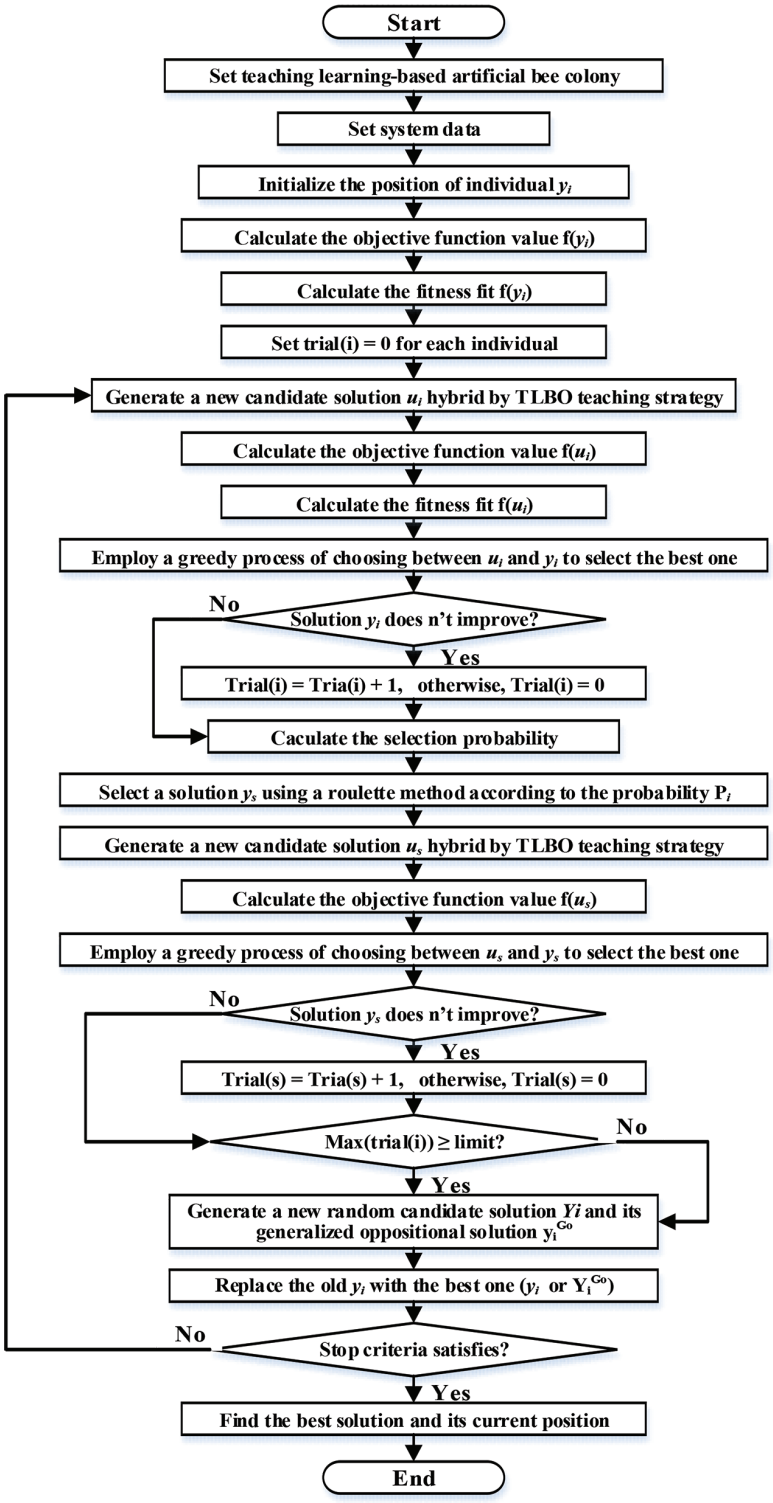

Figure 6. Flow chart of TLABC.

Table 1. Main results obtained by developed algorithm (69-node DS).

Item	Without DG	With DGs [size (kW)@location]		
		One DG	Two DGs	Three DGs
P_{loss} (kW)	224.97	83.222	71.647	69.426
Q_{loss} (kVAr)	102.19	40.568	35.949	34.968
Loss reduction (%)	-	63	68.14	69.14
V_{min} (pu@bus no.)	0.9092@	0.9683@ 27	0.9789@ 65	0.979@ 65
V_{max} (pu@bus no.)	0.99997 @ 2	1 @ 2	0.99997 @ 2	0.99998 @ 2
Total DG installations	-	1872.7@61	1781.5@61 531.48@17	370.3@18 508.44@11 1670.84@61
VSI	0.683	0.879	0.9183	0.9185
Losses cost ($)	118247	43741.69	37672.09	36490.06
Savings ($/year)	-	74505	80575	81757

667.448 kW, 574.875 kW and 516.2841 kW (with loss reduction of 21.66%,48.57%, 55.70% and 60.22%) when one, three, five and seven PV-based DG units are included, respectively. If we take the energy cost 0.06 $, the annual energy savings are $ 534374.435, $ 350810.436, $ 302154.346 and $ 271358.938 for integrated one, three, five and seven PV-based DG units in the test DS, respectively. The minimum voltage raised from 0.8688 p.u. up to 0.9053, 0.95410, 0.95413 and 0.95460 p.u for integrated one, three, five and seven PV-based DG units in the test DS, respectively. The minimum VSI raised from 0.5698 p.u. up to 0.6716, 0.8286, 0.83 and 0.8303 p.u for integrated one, three, five and seven PV-based DG units in the test DS, respectively.

As Table 4 shows, the developed approach allows the highest power loss reduction in case of installing seven DG units compared to other optimization approaches. Consequently, the developed approach is considered more effective and dependable compared with competitive optimization techniques regarding the overall power loss reduction in DS.

6.1.3. Comparison of statistical indicators of TLABC vs. GA and DE

On the whole, the heuristic techniques are distinguished by its randomness. Therefore, many tests have been performed to prove the robustness of the TLABC with 15 independent runs. The optimization OF's convergence curves of the three methods (i.e. TLABC, GA, and DE) of the Ploss are shown in Figures 7 and 8.

In comparison with GA and DE algorithms, the results show that the TLABC accelerates to the near optimal solution seamlessly, and in steady convergence characteristics. Also, the efficacy and robustness of the proposed TLABC over GA and DE algorithms are verified based on statistical factors, where many trials have been made. The minimum, maximum, mean, the standard deviation (SD) and average simulation time (AST) of the objective function after 15 runs for standard 69-node DS with integrating of three PVs with PLSF as presented in Table 5 and without PLSF as presented in Table 6.

These compressions used to check if the near-optimal solution located inside this limited search space or not. From these compressions, we can see the PLSF is suitable for the optimization problem.

The minimum, maximum, average, SD and AST of the objective function after 15 runs for standard 118-node DS with integrating of seven PVs using PLSF are presented in Table 7. In addition, the proposed

Table 2. Comparison between results of studied system obtained by different optimization methods (69-node DS).

Method	DG installed size(kW)@bus	Active power losses	
		Amount (kW)	Loss reduction(%)
Without DGs	-	224.97	-
BA [7]	2000@61 300@22 400@13	72.6	67.73
PSO [7]	700@66 1900@62 300@18	73.1	67.51
QOTLBO [6]	533.4@18 1198.6@61 567.2@63	71.625	68.17
QOSIMBO-Q [6]	831.4@9 453.8@17 1500@61	71	68.44
MINLP [9]	530@11 380@17 1720@61	69.59	69.07
KHA [10]	496.2@12 311.3@22 1735.4@61	69.563	69.08
SFSA [8]	527.3@11 380.5@18 1719.8@61	69.428	69.1389
GA	524.464@11 380.443@21 1712.2@61	69.488	69.113
DE	1730.7@61 339.05@18 536.63@11	69.486	69.115
TLABC	380.35@18 526.91@11 1718.8@61	69.426	69.1391

TLABC algorithm has more robust statistical indicators than the other algorithms, such as GA and DE. Similar indicators can be extended straightforwardly to other scenarios as well.

6.2. Scenario (2)

As mentioned above, BESs are installed at the determined PV locations and the developed approach is employed optimally planning of the PV+BES units output power at every hour with the aim of minimizing the energy

Table 3. Main results obtained by developed algorithm (118-node DS).

Item	Without DG	With DGs [size (kW)@location]			
		One DG	Three DGs	Five DGs	Seven DGs
P_{loss} (kW)	1297868	1016.694	667.45	574.875	516.284
Q_{loss} (kVAr)	978.65	776.065	508.667	432.572	393.736
Loss reduction (%)	-	21.664	48.574	55.706	60.221
V_{min} (pu@bus no.)	0.8688	0.9053@111	0.9541@54	0.95413@54	9546@54
V_{max} (pu@bus no.)	0.9959@2	0.99709@63	0.99791@100	0.99804@100	0.99815@2
Total DG installations	-	2978.6@71	2978.6@71 2883.3@50 2869.3@110	3119.7@109 1609.6@96 2478.8@72 2954.6@50 2088.3@80	2869.3@110 1154.3@42 2333.7@50 3708.2@30 2533.3@72 2094.9@80 1663.1@96
VSI	0.5698	0.6716	0.8286	0.83	0.8303
Losses cost ($)	682159	534374	350810	302154	271359
Savings ($)	-	147790	331350	380010	410800

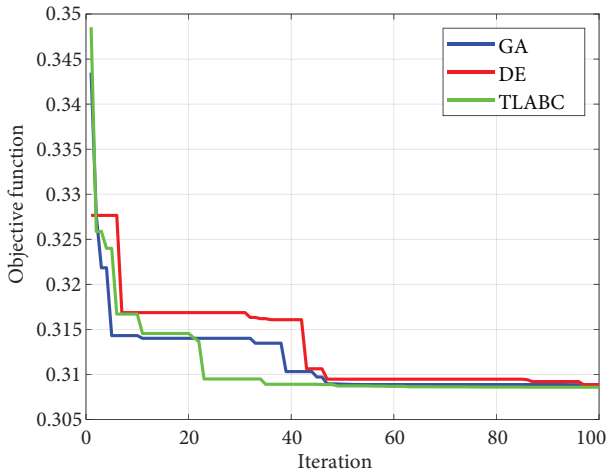

Figure 7. Power losses Convergence curves for different optimization methods (69-node DS).

losses. Using the output power curve of PV+BES, the optimal size of PV and BES can be achieved using the model described in Section 4.4. Figure 9 shows the PV+BES units output power curve at nodes 11, 28 and 61 of 69 node DS, respectively. These curves following the load demand curve in Figure 4, as PV+BES units are considered manageable resources.

Figure 10 shows the hourly output power of combined PV and PV+BES units at node 11. This PV unit's power output curve's obviously follows the expected PV model power output curve's as shown in Figure 4. From Figure 9, it can be observed that the maximum power output of the PV unit is determined at 12:00 h. and it is considered the optimal size of PV based DG. Also, it can be observed that the PV unit generates

Table 4. Comparison between results of studied system obtained by different optimization methods (118-node DS).

Method	DG installed size(kW)@bus	Active power losses	
		Amount (kW)	Loss reduction(%)
Without DGs	-	1297.868	-
KHA [10]	1724.2@48 1335.6@53 1862.3@74 1865.3@80 1663.1@96 1947.3@109 1184.8@112	574.71	55.73
SFSA [8]	1375.7@21 1199.7@42 2741.8@50 2891.5@71 1702.5@81 1332.1@97 2667.4@110	525.277	59.53
GA	3156.5@109 4590.5@30 1904.9@96 2189.4@50 1117.7@42 3181.9@71 1771.4@80	528.02	59.317
DE	1676.7@96 1595.2@22 1394.3@42 2395.8@72 2430.1@81 2379.4@50 3221.2@110	530.31	59.13
TLABC	2869.3@110 1154.3@42 2333.7@50 3708.2@30 2533.3@72 2094.9@80 1663.1@96	516.28	60.221

the energy against to PV+BES unit energy accommodated by the system to keep power loss minimum at each time. The hourly differences between the two curves determine the discharge and charge energy of the BES

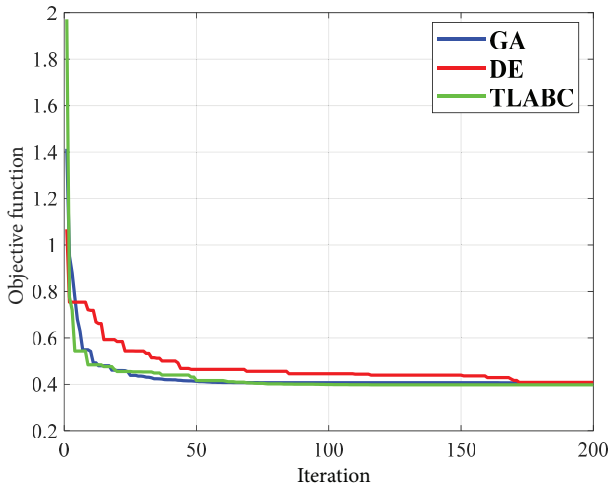

Figure 8. Power losses Convergence curves for different optimization methods (118-node DS).

Table 5. Statistical analysis for GA, DE and TLABS regarding power losses with PLSF (69-node DS).

Method	Best solution	Average solution	Worst solution	SD	Average simulation time
GA	69.488	71.609.78	73.17.4	1.0137	9.863
DE	69.487	69.698.5	69.947	0.1649	9.843
TLABC	69.425	69.619.9	69.842	0.2086	10.812

Table 6. Statistical analysis for GA, DE and TLABS regarding power losses without PLSF (69-node DS).

Method	Best solution	Average solution	Worst solution	SD	Average simulation time
GA	70.476	71.891	73.055	1.0137	10.202
DE	69.525	70.086	70.811	0.1649	9.9172
TLABC	69.426	69.577	69.95	0.2086	11.952

Table 7. Statistical analysis for GA, DE and TLABS regarding power losses with PLSF (118-node DS).

Method	Best solution	Average solution	Worst solution	SD	Average simulation time
GA	528.016	543.035	566.97	15.856	71.577
DE	530.31	545.764	558	9.6638	51.602
TLABC	516.284	525.184	541.098	9.2091	79.569

unit. Using the power output of PV + BES, the optimal size for PV and BES can be achieved using PV+BES model.

The maximum power output difference between PV and PV+BES units is found at 13:00, which provides the maximum charging power or the nominal power rating of the BES unit (P_{BES}). Similarly, for the reminder

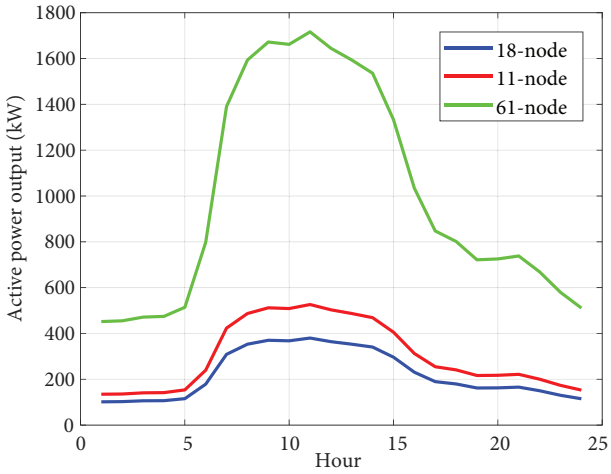

Figure 9. Daily PV+BES output power curves in different positions of 69 node DS.

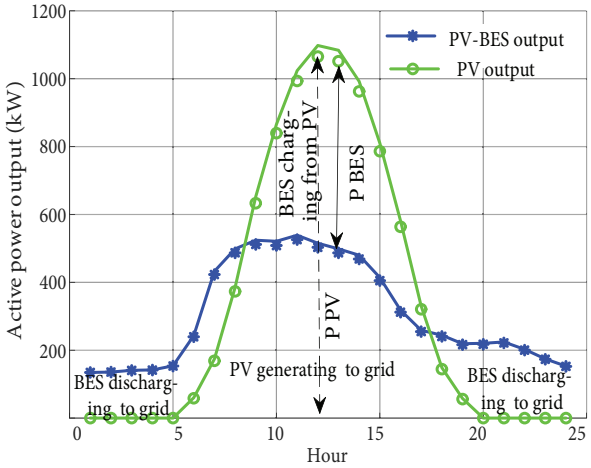

Figure 10. PV and PV+BES output power curves at node 11.

units connected at nodes, the results are obtained. Tables 8 and 9 are presents the results for the PV unit's sizes as well as the nominal power and power output of the BES units for 69 node and 118 node DSs. In addition, Figures 11 and 12 show the effect of three PV+BES units' installation on the voltage profile of 69 node system.

Table 8. Optimal size and location of PV+BES in 69-node DS.

Location	Node 11	Node 18	Node 61	Total
PV size (kW)	1065.46	783.78	3517.4	5366.6
BES rated power (kW)	564.6	420.5	1878.3	2863.4
BES energy capacity (kWh)	3220	2401.9	10723	16344.8

Table 9. Optimal size and location of PV+BES in 118-node DS.

Location	Node 109	Node 96	Node 72	Node 50	Node 80	Total
PV size (kW)	6355.56	3408.73	5171.45	5919.46	4298.98	25154.2
BES rated power (kW)	3384.32	1822.43	2757.67	3168.18	2300.14	13432.73
BES energy capacity (kWh)	19308.61	10403.16	15736.37	18087.9	13131.47	76667.51

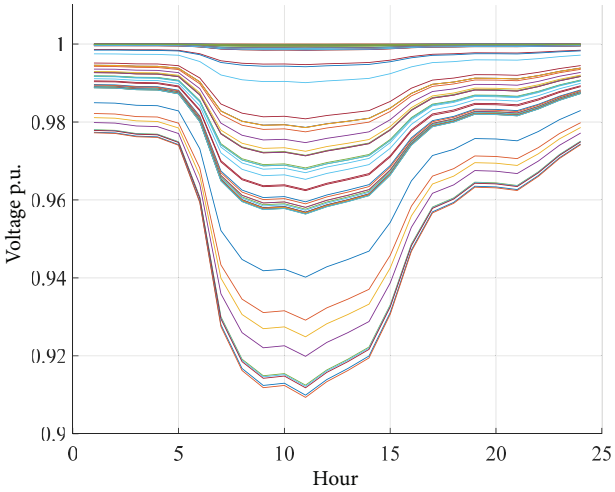

Figure 11. Impact of three DG installations on voltage profile of 69-node DS without BES integration.

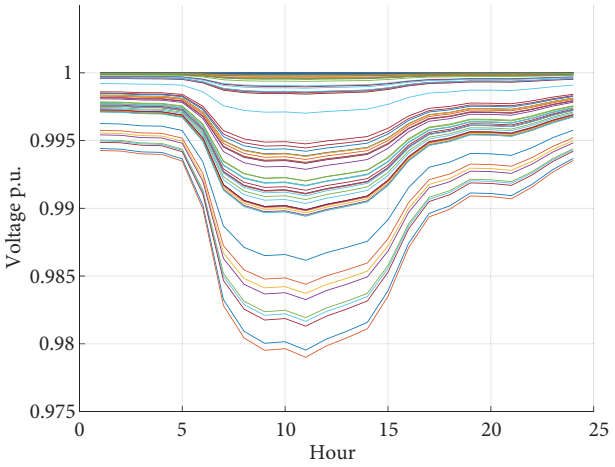

Figure 12. Impact of three DG installations on voltage profile of 69-node DS with BES integration.

6.3. Energy losses analysis

Figure 13 shows the results of power losses of the base case and the impact of PV and PV+BES installation on the DS active losses. A noticeable decrease in energy loss in Scenario 2 is observed when compared with the base case. Total energy losses and their loss reduction for the studied day are presented in Tables 10 and 11 for 69 node and 118 node DSs. The maximum reduction in energy loss is 68.34% and 0.5483% for 69-node and 118-node DSs, respectively.

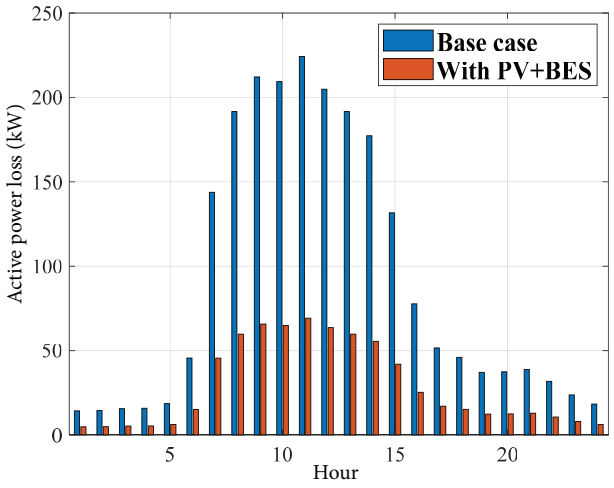

Figure 13. Impact of three DG installations on active power losses of 69-node DS.

Table 10. Daily energy losses of 69-node DS.

Scenario	Energy loss (kWh)	Loss reduction %
Base case	2173.85	-
With PV+BES	688.13	68.34

Table 11. Daily energy losses of 118-node DS.

Scenario	Energy loss (kWh)	Loss reduction %
Base case	12535.016	-
With PV+BES	5661.857	54.83

7. Conclusion

In this study, a hybrid TLABC optimization method with PLSF has been developed to find the optimal location and sizing of single and multiple PV and three PV+BES units for 69 node and five PV+BES units for 118 node DSs, taking into account uncertainties in power generation and time-varying load. The Beta PDF models are employed to depict the randomness of solar radiation. The OF is designed to minimize the overall energy losses of DS. The performance of the developed approach has been tested on the 69-node and large-scale 118-node DSs. Three PV and PV+BES units for 69 node and five PV and PV+BES units for 118 node DSs have been realized to test the capabilities of developed approach to minimize the total energy losses and impact of them to the voltage profile. The performance of developed approach has been compared with GA and DE based on statistical analysis as well as other optimization techniques in the literature. The results showed that the developed approach is more effective than many other algorithms in minimizing the total power losses.

Acknowledgment

The authors would like to acknowledge the support of the Chilean Council of Scientific and Technological Research, ANID/Fondap/15110019.

References

[1] Hurlbut D. Stage Clean Energy Practices: Renewable Portfolio Standards. National Renewable Energy Laboratory Technical Report. Washington, DC, USA: U.S. Department of Energy, 2008.

[2] Omran WA, Kazerani M, Salama MMA. Investigation of methods for reduction of power fluctuations generated from large grid-connected photovoltaic systems. IEEE Transactions on Energy Conversion 2010; 26: 318-327.

[3] Celik AN. Optimisation and techno-economic analysis of autonomous photovoltaic–wind hybrid energy systems in comparison to single photovoltaic and wind systems. Energy Conversion and Management 2002; 43: 2453-2468.

[4] Kansal S, Kumar V, Tyagi B. Hybrid approach for optimal placement of multiple DGs of multiple types in distribution networks. International Journal of Electrical Power and Energy Systems 2016; 75: 226-235.

[5] Ganguly S, Samajpati D. Distributed generation allocation with on-load tap changer on radial distribution networks using adaptive genetic algorithm. Applied Soft Computing 2017; 59: 45-67.

[6] Sharma S, Bhattacharjee S, Bhattacharya A. Quasi-oppositional swine influenza model based optimization with quarantine for optimal allocation of DG in radial distribution network. International Journal of Electrical Power and Energy Systems 2016; 74: 348-373.

[7] Prakash R, Sujatha BC. Optimal placement and sizing of DG for power loss minimization and VSI improvement using bat algorithm. In: 2016 National Power Systems Conference; Bhubaneswar, India; 2016. pp. 1-6.

[8] Nguyen TP, Vo DN. A novel stochastic fractal search algorithm for optimal allocation of distributed generators in radial distribution systems. Applied Soft Computing 2018; 70: 773-796.

[9] Kaur S, Kumbhar G, Sharma J. A MINLP technique for optimal placement of multiple DG units in distribution systems. International Journal of Electrical Power and Energy Systems 2014; 63: 609-617.

[10] Sultana S, Roy PK. Krill herd algorithm for optimal location of distributed generator in radial distribution system. Applied Soft Computing 2016; 40: 391-404.

[11] Khasanov M, Xie K, Kamel S, Wen L, Fan X. Combined tree growth algorithm for optimal location and size of multiple DGs with different types in distribution systems. In: 2019 IEEE Innovative Smart Grid Technologies-Asia; Chengdu, China; 2019. pp. 1265-1270.

[12] Mikati M, Santos M, Armenta C. Electric grid dependence on the configuration of a small-scale wind and solar power hybrid system. Renewable energy 2013; 57; 587-593.

[13] Bayod-Rujula AA, Haro-Larrodé ME, Martinez-Gracia A. Sizing criteria of hybrid photovoltaic–wind systems with battery storage and self-consumption considering interaction with the grid. Solar Energy 2013; 98; 582-591.

[14] Alam MJ, Muttaqi KM, Sutanto D. Mitigation of rooftop solar PV impacts and evening peak support by managing available capacity of distributed energy storage systems. IEEE Transactions on Power Systems 2013; 28: 3874-3848.

[15] Sugihara H, Yokoyama K, Saeki O, Tsuji K, Funaki T. Economic and efficient voltage management using customer-owned energy storage systems in a distribution network with high penetration of photovoltaic systems. IEEE Transactions on Power Systems 2012; 28: 102-111.

[16] Teng JH, Luan SW, Lee DJ, Huang YQ. Optimal charging/discharging scheduling of battery storage systems for distribution systems interconnected with sizeable PV generation systems. IEEE Transactions on Power Systems 2012; 28: 1425-1433.

[17] Deb K. An introduction to genetic algorithms. Sadhana 1999; 24: 293-315.

[18] Storn R, Price K. Differential evolution–a simple and efficient heuristic for global optimization over continuous spaces. Journal of Global Optimization 1997; 11 (4):341-359.

[19] Kamel S, Awad A, Abdel-Mawgoud H, Jurado F. Optimal DG allocation for enhancing voltage stability and minimizing power loss using hybrid gray wolf optimizer. Turkish Journal of Electrical Engineering and Computer Sciences 2019; 27 (4): 2947-2961.

[20] Ali ES, Abd Elazim SM, Abdelaziz AY. Ant lion optimization algorithm for renewable distributed generations. Energy 2016; 116: 445-458.

[21] Murthy VV, Kumar A. Comparison of optimal DG allocation methods in radial distribution systems based on sensitivity approaches. International Journal of Electrical Power and Energy Systems 2013; 53: 450-467.

[22] Arya LD, Koshti A, Choube SC. Distributed generation planning using differential evolution accounting voltage stability consideration. International Journal of Electrical Power and Energy Systems 2012; 42 (1): 196-207.

[23] Hung DQ, Mithulananthan N, Bansal RC. Integration of PV and BES units in commercial distribution systems considering energy loss and voltage stability. Applied Energy 2014; 113: 1162-1170.

[24] Hung DQ, Mithulananthan N, Lee KY. Determining PV penetration for distribution systems with time-varying load models. IEEE Transactions on Power Systems. 2014 Apr 14; 29 (6): 3048-57.

[25] Rao RV, Savsani VJ, Vakharia DP. Teaching–learning-based optimization: a novel method for constrained mechanical design optimization problems. Computer-Aided Design 2011; 43 (3): 303-315.

[26] Karaboga D, Basturk B. A powerful and efficient algorithm for numerical function optimization: artificial bee colony (ABC) algorithm. Journal of Global Optimization 2007; 39 (3): 459-471.

[27] Chen X, Xu B. Teaching-learning-based artificial bee colony. International Conference on Swarm Intelligence. Cham, Switzerland: Springer, 2018, pp. 166-178.

[28] Savier JS, Das D. Impact of network reconfiguration on loss allocation of radial distribution systems. IEEE Transactions on Power Delivery 2007; 22 (4): 2473-2480.

[29] El-Fergany AA, Abdelaziz AY. Capacitor allocations in radial distribution networks using cuckoo search algorithm. IET Generation, Transmission and Distribution 2014; 8 (2): 223-232.